Increasing spatial resolution of 3D LiDAR by Compressive Sensing

Erwan Viala, Nicolas Rivière, Laurent Risser, Paul-Édouard Dupouy

INCREASING SPATIAL RESOLUTION OF 3D LIDAR BY COMPRESSIVE SENSING

Viala Erwan* [(1)], Rivière Nicolas [(1)], Risser Laurent [(2)], Dupouy Paul-Édouard [(1)]

[(1)] ONERA\DOTA, Toulouse University, FR 31055 Toulouse, France
[(2)] Toulouse Mathematics Institute, UMR CNRS 5219, Toulouse, France
** erwan.viala@onera.fr*

KEYWORDS: LiDAR, GmAPD, Compressive Sensing, 3D focal plane array, long-range imagery

ABSTRACT

ONERA – The French Aerospace Lab – develops new concepts of LiDAR imaging systems including new sensor technologies and data processing. The rising complexities and costs of high performance systems, and the shrinking time to design drove the ONERA approach. The home-grown MATLIS software has been evolving for the past decade. It allows both linear mode LiDAR and single photon electro-optical systems simulation (both GmAPD and SPL) embedded on dynamic platforms (*eg*. UAVs, Aircrafts).

In this paper, we present an algorithm for 3D scene reconstruction with unprecedented lateral resolution. This method is suitable for Geiger mode Avalanche Photodiode (GmAPD) 3D focal plane arrays. The main idea behind of this work is reconstruction of higher resolution 3D images by sub-pixel spatial modulation.

We manage to reconstruct sub-pixel information by using Compressive Sensing (CS) algorithms, such as Orthogonal Matching Pursuit (OMP). Then we have verified our theoretical approach using simulated 3D images generated using the MATLIS software from a facetted three-dimensional scene.

1. INTRODUCTION

1.1. Context and motivation

Long-range observation typically above 10 kilometers, is necessary to anticipate potential threats for site surveillance (*eg*. drone detection) or aerial / maritime protection (*eg*. identification of floating debris, ship self-protection). The operational needs of these tasks require a persistence of the detection and identification function under any weather and illuminance conditions (*eg*. day, night, sun glare). In this context, one can notice that passive imagery techniques (visible or infrared) answer partially to the identification function. Operational deployment especially in weak visibility or strong solar illuminance variation in time as proven to be challenging. Active imaging as illustrated in Fig. 1 is less sensitive to it by the use and control of its own illumination source. Moreover, the identification function needs a good lateral and telemetric resolution and the image telemetry bring additional dimension which eases the identification.

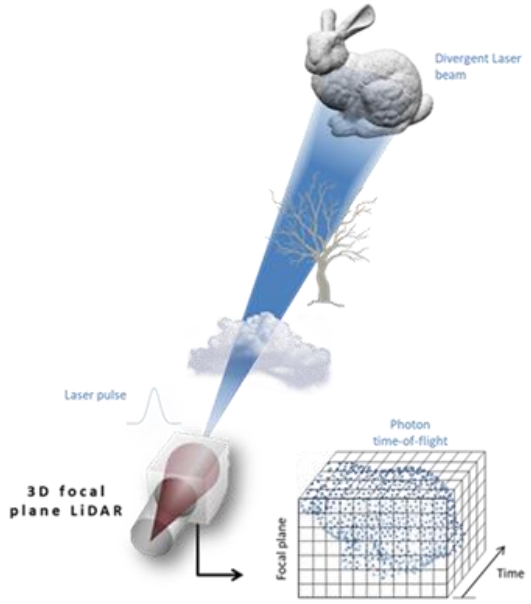

Figure 1 – Concept of 3D LiDAR acquisition based on focal plane array.

Active imaging is governed by the capacity to capture laser-light backscattered by a target. The combined need for range, resolution and reduced SWaP (Size, Weight and Power) mandates the use of a specific sensor to image the scene. In this case, we focus on systems using GmAPD sensor, capable of statistically detecting fractional photons return levels. These sensors have some drawbacks. GmAPDs are limited to a few large pixels (up to 128x32 pixels), which gives an insufficient resolution for the identification function. In section 2, we will show how this can be alleviated by using CS to increase the resolution at the cost of a spatial modulator and a fast algorithm.

Moreover, those sensors, in gated mode, are only capable of capturing the first triggering event. The low dynamic range and temporal correlation complicate the application of CS to such a 3D imagery. In section 3, we will explain these difficulties in more detail and our approach to solve

them. Then in section 4 we illustrate, our approach by reconstruct with increased resolution an image at a range of 10 km on simulated data.

2. COMPRESSIVE SENSING

2.1. General concept

CS can be considered as an acquisition technique that compresses the signal during the acquisition process in order to acquire already compressed information and then uses of a L^1 optimization algorithm to reconstruct the acquired information.
The main concepts of CS were developed between 2005 and 2009 by three mathematicians (Candès, Tao and Romberg) [1-3] and in parallel by Donoho since 2006 [4]. CS uses the sparsity of the scene on a certain basis (which may be unknown) and the inconsistency between this basis and a specific measurement basis to enable the correct reconstruction of the image.

Theorem (2K-RIP): [1,2]
Let Φ follow the $2k$- Restricted Isometry Property if for $k < N, \exists \delta_{2k} \in$, such that :

$$(1 - \delta_{2k})\|X\|^2 \leq \|\Phi_{2k}X\|^2 \leq (1 + \delta_{2k})\|X\|^2 \quad (1)$$

For all Φ_{2k} composed of $2k$ columns extracted from Φ.

Thus, from the 2K-RIP (Eq. 1), we have two resulting restrictions: the signal must be sparse in a basis Ψ which may be unknown, and the measurement matrix Φ must be sufficiently inconsistent with the basis Ψ.

Theorem (Noisy recovery with bounded noise): [3]
If $\delta_{2k} \leq \sqrt{2} - 1$, then

$$\|x_0 - x^\star\| \leq \frac{C_0}{\sqrt{k}}\|x_0 - x_k\|_1 + C_1\varepsilon \quad (2)$$

where x_k is the best k–term approximation of x_0, $x^\star$ is the reconstructed signal and C_0, C_1 are related to δ_{2k} and are rather small.

According to Eq. 2, this property is sufficient to guarantee a limited error on the reconstruction.

In our case, we choose the two most commonly used bases in LiDAR application (especially in single pixel imaging), which are the random basis composed of multiple Bernoulli, and the Hadamard basis, which is determinist. The Random basis or Hadamard basis (Fig. 2), which are respectively incoherent with all basis with high probability and with basis like Haar or Daubechies in which the natural scene is generally sparse. [5]

Figure 2 - Bases examples

2.2. 3D LiDAR Application

We use DMD (Digital Micro-mirror Device) to compress backscattered signal in 3D LiDAR application as illustrated in Fig. 3.

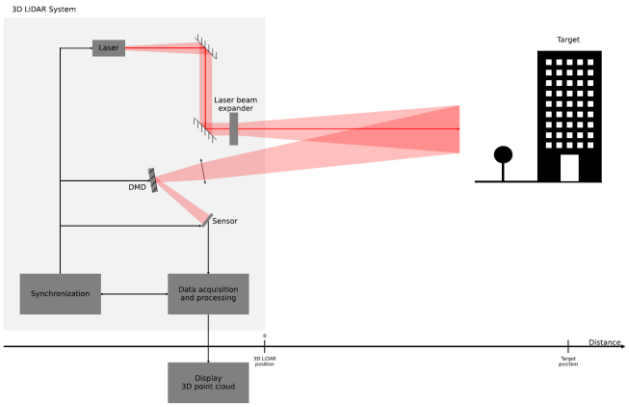

Figure 3 - Optical scheme

A DMD is an array of mirrors which are orientable (Fig. 4 and Fig. 5), so we can structure the detection by directing the light to the sensor or not. Then we can easily compress the signal with basis composed of zero and one, like the example in Fig. 2.

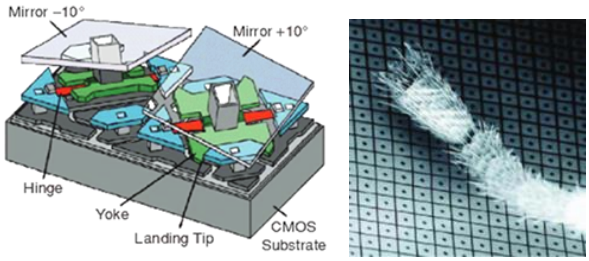

Figure 4 – Left: two mirrors from a Texas Instrument DMD. Right: DMD with ant-leg for scale

Thus, we compress our signal with a DMD. One need to make additional assumptions to process a suitable signal for CS. Each pixel is supposed to be spatially and temporally independent of its neighbors. This assumption is needed to reconstruct independently three-dimensional objects in each temporal bin of each pixel. We also assume that the signal is time-dependent but not pattern-dependent, which is not the case, in section 3.2 we developed a way to solve this issue.

Then, we acquire the 3D-LiDAR data with measurement basis according to CS theory, adjust the data and finally reconstruct the image by solving the CS optimization problem with classical algorithm like Orthogonal Matching Pursuit (OMP) [6].

3. PRECOMPUTATION STAGE

When we deal with CS in LiDAR GmAPD imaging, we encounter at least two major problems as already mentioned in sections 1 and 2:

- Low dynamics
- Time-dependency

In this section we will briefly aboard a way to deal with them.

3.1. Low dynamics

The first problem is the lack of dynamics of the sensor. Because of high dead-time and the high sensitivity of the sensor, the output from the sensor is limited to the information that an event (backscattered photon or noise) is detected at a time, only for the first trigger (for each pixel) and without information about the number of photons.

Therefore, a classical way to deal with this problem is to use a histogram of return time to infer the quantity of photon which could be counted at each bin of each pixel.

The error can be bounded by using the Hoeffding inequality [7], as follow (Eq. 3):

$$|H - Y| \leq \sqrt{\frac{ln\left(\frac{2}{\alpha}\right)}{2N}} \qquad (3)$$

Where H is the normalized histogram, Y is the measure expected, $1-\alpha$ is the level of trust and N is the number of acquisition.

Once this method is applied, we get an error-bound approximation of the signal waveform for each pixel.

3.2. Time-dependency

The time-dependency is a more involved problem. It is linked with the pattern-dependency. Of course the signal depends on time since it decreases quadratically with time, but it's also pattern dependent which is the real problem. This effect is illustrated in fig. 6.

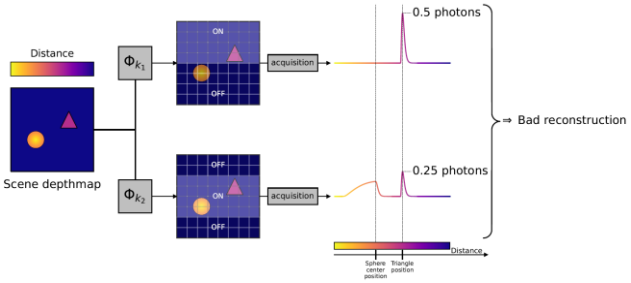

Figure 6 - Illustration of time-dependency error

For a given pattern the more of an object is exposed the more signal we should have. It's not always the case because it depends on the quantity of object seen before the bin of interest. This error will lead to a mismatch between the weight applied on the pattern and the quantity of the shape exposed. Thus, when an object is detected in a bin, all the following bins could have wrong weight which could be a problem when solving the CS optimization problem.

To overcome this problem, we just reweighed each bin with a coefficient, which depends of the previous bins. This coefficient is obtained by making some assumption about the probability of return in each point. This observation is experimentally validated by [8], on the same kind of sensor.

Another problem which comes with this method is the presence of noise. When we apply the weigh to reweigh all bins, noise is highly amplified. In order to avoid a too noisy reconstruction, we must use a denoiser.

4. SIMULATED RESULTS

In order to test our algorithm, we have used simulated 3D LiDAR acquisitions by MATLIS software [9].

4.1. Input parameters for MATLIS software

The simulation parameters used are chosen to be as realistic as possible. The laser energy is around 10^{-5}Jand the total noise (solar + dark count rate) around $10^{6}\mathrm{Hz}$ as in daylight conditions. The sensor is placed at a range of $10\mathrm{km}$ of the scene with a field of view around 10^{-4} rad which is equivalent at a $5\mathrm{m}$ by $5\mathrm{m}$ square at $10\mathrm{km}$. The Geiger focal plane is composed by 32×32 pixels and the DMD by 256×256 mirrors. The frame rate and DMD pattern update-rate correspond to realistic parameters.

4.2. Results

The 3D scene was designed to illustrate the improvement brought by the method (Fig. 7a).
In Fig. 7b and Fig. 7c, colors represent the normalized intensities, after the histogram of time return (Fig. 7b) and reconstruction with CS (Fig. 7c). Considering the biggest and less detailed objects, the improvement for recognition is not high ('ONERA' letters), even though borders are slightly better defined. The French motto is unreadable in Fig. 7b but it's pretty clear in Fig. 7c. The bust of the French Marianne is also better defined.

(a)

(b) (c)

Figure 7 - (a) Original scene, (b) 3D point cloud of a LiDAR (noise removed) and, (c) reconstruction including CS post-processing

CONCLUSION

In this paper we describe a new theoretical 3D LiDAR process based on compressive sensing. We use simultaneously a focal plane array in Geiger mode and a CS approach based on DMD. We have highlighted the fact that this application is not trivial. We also developed an algorithm using signal processing and then CS with OMP to achieve a 3D reconstruction. The resolution of the final image is increased at long range (<10 km) under realistic daylight conditions.

5. ACKNOWLEDGMENTS

The authors would like to thank the Région Occitanie for funding this research through a doctoral fellowship**.**

6. REFERENCES

1. E. J. Candes, J. Romberg and T. Tao. (2006) Robust uncertainty principles: exact signal reconstruction from highly incomplete frequency information. in *IEEE Transactions on Information Theory*, **52(**2), 489-509.
2. E. J. Candès and T. Tao. (2006). Near-Optimal Signal Recovery From Random Projections: Universal Encoding Strategies? in *IEEE Transactions on Information Theory*. **52**(12), 5406-5425.
3. A. Zymnis, S. Boyd and E. Candes. (2010) Compressed Sensing With Quantized Measurements, in *IEEE Signal Processing Letters*. **17**(2), 149-152
4. Donoho, D. L. (2006). Compressed sensing. *IEEE Transactions on information theory*, **52**(4), 1289-1306.
5. Antun, Vegard. (2016) Coherence estimates between hadamard matrices and daubechies wavelets*. MS thesis*
6. Pati, Y. C., Rezaiifar, R., & Krishnaprasad, P. S. (1993). Orthogonal matching pursuit: Recursive function approximation with applications to wavelet decomposition. In *Proceedings of 27th Asilomar conference on signals, systems and computers IEEE* , 40-44
7. Wasserman, L. (2013). All of statistics: a concise course in statistical inference. *Springer Science & Business Media.*
8. M. E. O'Brien et D. G. Fouche, (2005) Simulation of 3D laser radar systems, Lincoln Laboratory Journal, **15** (1), 37–60
9. G. Anna, L. Hespel, N. Riviere, D. Hamoir and B. Tanguy. (2010) Physical modelling of point-cloud (3D) and full-wave-form (4D) laser imaging*, Proceedings of SPIE - The International Society for Optical Engineering*, **7835**